Nuclear Instruments and Methods in Physics Research A266 (1988) 550–559
North-Holland, Amsterdam

Section IV. Research instrumentation: (a) Particle analysers and detectors

ELECTRON SPIN POLARIZATION ANALYZERS FOR USE WITH SYNCHROTRON RADIATION

D.T. PIERCE, R.J. CELOTTA, M.H. KELLEY and J. UNGURIS

National Bureau of Standards, Gaithersburgh, MD 20899, USA

The measurement of the spin polarization of photoelectrons emitted from a magnetic material is discussed. An important consideration is the acceptance phase space of the spin analyzer relative to the phase space of the photoemitted electrons to be measured. Other considerations include the magnetization direction relative to the extracted beam and whether the measurements are angle integrated or angle resolved. In the longitudinal geometry where the magnetization is normal to the sample surface and along the extracted photoelectron beam, conservation of canonical angular momentum adds an additional magnetic term to the beam emittance which is absent when the magnetization is in the sample plane and transverse to the extracted beam. For angle resolved measurements in the transverse geometry, the advantages of a new, low-energy (~100 eV) spin analyzer which is easily movable, compact and efficient are discussed. Different spin analyzers are described and compared, and an analysis of their application to different spin polarized photoemission measurement configurations is given.

1. Introduction

A wealth of information about the electronic structure of solids and surfaces has been obtained from ultraviolet photoemission spectroscopy (UPS) and X-ray photoemission spectroscopy (XPS) using synchrotron radiation. When the spin polarization of the photoemitted electrons is measured, this information is extended to include the spin dependent electronic structure of a magnetic material [1]. The magnetization depends on the net spin density in the ferromagnetic material. Since the electron spin polarization is generally conserved in the photoemission process, a spin-polarized photoemission measurement determines the energy (and momentum) distribution of magnetic states in a solid. For example, the observation of the spin-split energy bands of Fe as a function of temperature has provided insight onto the fundamental description of finite temperature magnetism [2]. Without a spin polarization measurement, the identification of spin-dependent features in an angle resolved photoemission spectrum by relying on band structure calculations can be ambiguous and lead to incorrect conclusions [3]. The problem is compounded in the case of surface states where calculations are more difficult.

The opportunities for landmark investigations of magnetic properties by spin-polarized UPS and XPS are numerous. A number of spectral peaks in spin-integrated photoemission studies of ferromagnetic surfaces have been attributed to magnetic surface states, but await conclusive testing by measurement of the spin polarization. Even in a nonferromagnetic material like antiferromagnetic Cr, energy-split peaks in a photoemission spectrum of the Cr(100) surface have been attributed to ferromagnetism at the surface and the resulting exchange splitting of the states [4]. The origin of the energy-split surface peaks can be conclusively determined by spin-polarized photoemission.

Spin analysis combined with XPS can give an element specific measure of the local magnetism. The photoelectrons are polarized due to exchange interaction between valence electrons and core states. Spin analysis coupled with the elemental specificity of XPS may be used to probe the magnetism at an interface and, by varying the X-ray photoelectron kinetic energy, the depth profile of the magnetization can be determined.

There have been many advances lately in the atomic engineering of materials by atomic and molecular beam epitaxial growth to achieve magnetic materials of altered crystal structure or lattice constant [5]. Growing a ferromagnetic material with increased lattice constant is like applying negative pressure which increases the magnetic moment and the tendency to ferromagnetism. Advances in theory and computation enable predictions to be made [6] of the magnetic properties of a variety of thin film/substrate systems which can now be physically realized and which would be interesting to test experimentally.

The spin analyzer is central to any of these measurements. Although there have been significant improvements in reducing the size and thereby increasing the convenience of operation of spin analyzers, the fact remains that spin analyzers are terribly inefficient. For example, in the measurement of the spin polarization $P \pm \Delta P$ of a beam comprised of N_0 electrons, the uncertainty or error ΔP is [7]

$$\Delta P = \frac{1}{\sqrt{\mathscr{I} N_0}}, \tag{1}$$

where $\mathscr{F}$, the figure of merit of the spin analyzer, is further discussed below. The figure of merit obtained even in the best spin analyzers is only about 10^{-4}. In the case of measurement of the intensity of a beam of N_0 electrons, the relative uncertainty $\Delta N_0/N_0$ is $1/\sqrt{N_0}$. The relative uncertainty $\Delta P/P$ of the polarization is $(P^2 \mathscr{F} N_0)^{-1/2}$ so we see that for $|P| < 1$ it takes over 10^4 times as long to measure the degree of spin polarization of an electron beam as it does to measure its intensity.

In view of this low efficiency of spin analyzers, improvements in sources of synchrotron radiation are especially important. Sources of synchrotron radiation have evolved from the parasitic use of high energy physics storage rings to dedicated storage rings, and from bending magnet radiation to radiation from insertion devices such as wigglers and undulators. Third generation synchrotron radiation sources comprising optimized storage rings with low emittance electron beams and long straight sections for insertion devices are expected to achieve four orders of magnitude increase in photon brilliance [photons/(s mrad^2 mm^2 0.1% BW)] over present bending magnet sources [8]. The high brilliance which can be obtained from an undulator can substantially offset the low efficiency of an electron spin polarization analyzer. Spin polarized photoemission studies, carried out to date using bending magnet radiation, have already proven very valuable and point to the enormous opportunities for spin polarized photoemission with insertion devices and improved spin analyzers.

The organization of the rest of this article is as follows. In the next section, the experimental configurations for spin polarized UPS and XPS are described. In section 3 some electron optical phase space conservation principles are presented. The emittance of the sample in different experimental configurations and the acceptance of the energy analyzer are discussed along with the constraints they place on a spin analyzer. In section 4, several spin analyzers are described. Quantitative factors such as figure of merit and electron optical acceptance are described along with other factors such as size, stability, vacuum requirements, and apparatus asymmetries. Section 5 concludes with a brief discussion of the selection of spin analyzers depending on experimental configuration.

2. Experimental configurations

A ferromagnet tends to lower its free energy by breaking up into small regions or domains of magnetization which typically range in size from hundreds of nm to hundreds of μm. The direction of magnetization is uniform within a domain but can reverse in going from one domain to the next. If the beam of synchrotron radiation intercepts several domains, the polarization of photoemitted electrons will average to zero. There are two ways to overcome this. First, if the beam of radiation can be focused to an area smaller than a domain, as is done in scanning electron microscopy with polarization analysis (SEMPA) [9], the magnetic properties can be measured. With well focused synchrotron radiation, particularly that from undulators on low emittance storage rings impinging on magnetic targets with sizeable domains, spin polarized photoemission measurements may be possible provided the position of the incident radiation is very stable and can be controlled.

A second, more practical and generally applicable method, is the one used in spin polarized photoemission measurements to date. In this method one applies a magnetic field to the sample so as to magnetize it uniformly, such that the sample presents a single domain to the incident radiation. In vacuum, the electron trajectories spiral around lines of magnetic induction. Two experimental strategies are employed in two different configurations. In one, the magnetic induction outside the sample is minimized by magnetizing it in the plane of the photoemitting surface as in fig. 1a, the transverse configuration. In the other, the sample is magnetized perpendicular to the photoemitting surface as in fig. 1b, such that the electrons are extracted along the magnetic induction B (the longitudinal configuration).

In the transverse configuration a c-shaped electromagnet, typically with a soft-iron core, is used to magnetize the sample which acts as the keeper of the electromagnet and minimizes stray fields [10]. Ideally, the electromagnet and sample are all one continuous piece of material, for example a crystal in a picture frame shape [11]. The magnetic field, H, inside the sample is continuous across the surface and falls off rapidly away from it [12]. The polarization is along the axis defined by the magnetic field so there is no precession or consequent depolarization. To minimize the field required, it is desirable to magnetize the sample along an easy axis of magnetization. In the case of a thin film, the stray field due to the poles at the edge is small so that the iron core is not required to close the magnetic circuit and may be removed.

In the longitudinal configuration, even though the electrons spiral around lines of magnetic induction, some of the lines are along the axis, and electrons near the axis are extracted. Since B is continuous across the surface, B remains in the extraction region even with the sample magnetized in the remanent state. As the electron is accelerated out of the high field region, the transverse components of momentum cause the electrons to have skew trajectories. Angular information is lost, making angle-resolved measurements impossible in this configuration. The significant advantage of this

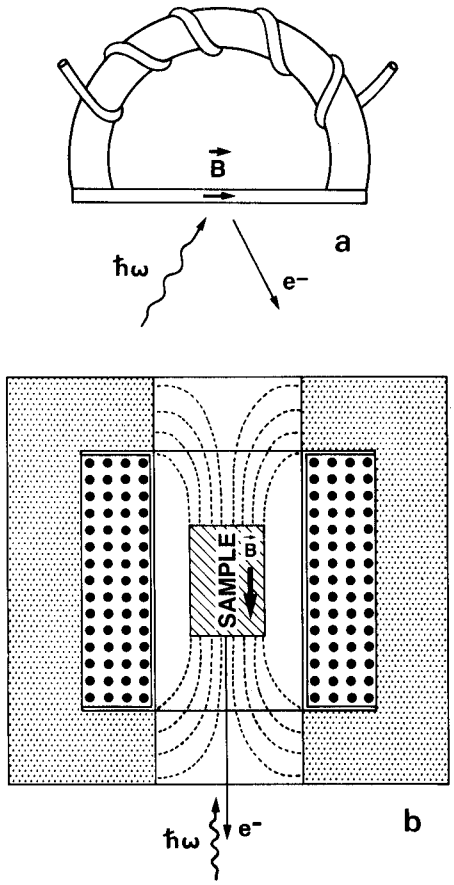

Fig. 1. Experimental configurations for spin polarized photoemission: (a) transverse geometry, and (b) longitudinal geometry. In (b), an iron housing around the electromagnet provides a return path for the magnetic field.

configuration is the possibility of measuring in a large magnetic field. This allows one to overcome the effects of magnetic anisotropy and magnetize along a hard axis or to measure out-of-plane magnetization [1]. UPS or XPS can be done in either the transverse or longitudinal configuration.

3. Electron optical phase space

3.1. Conservation laws

Some rather general ideas about phase space allow us to analyze the overall experimental system. For example, the envelope of the electron beam emitted from a photocathode encloses a certain volume of phase space. Both the energy analyzer and spin analyzer accept a limited volume of phase space. If this volume is less than that determined by the photocathode, some electrons will be lost. The best choice of a spin analyzer is one that is optimized for a given experiment. This will involve considering the phase space of the photocathode, the acceptance of the energy analyzer, and then choosing the spin analyzer to have sufficient acceptance to avoid any loss of beam.

The generalized Liouville theorem on the conservation of volume in the phase space defined by coordinates and conjugate momenta can be simplified for a paraxial electron optical system of macroscopic electric and magnetic fields in which the electron current is conserved. This simplification takes the form of the law of Helmholz–Lagrange, which states that for any two points 1 and 2 along a beam path, there is a conservation of the product of the energy E, the solid angle Ω, and cross sectional area A [13]:

$$E_1 A_1 \Omega_1 = E_2 A_2 \Omega_2 . \tag{2}$$

Frequently one refers to the emittance ϵ of an electron beam which is defined as

$$\epsilon = r\alpha , \tag{3}$$

where r is the radius (for example at the minimum in the envelope), and α is the half-angle formed by the asymptotic ray of the envelope. Noting that $\pi^2 \epsilon^2 = A\Omega$, we see that $\epsilon^2 E$ is a conserved quantity.

3.2. The photocathode emittance

The electron beam phase space volume at the sample, i.e. photocathode, in the transverse configuration is just $EA\Omega$, the product of the photoelectron energy, the emitting area, and the solid angle into which the electrons are emitted. In the longitudinal configuration, the magnetic field introduces a further contribution to the phase space. An abbreviated discussion of this follows; details have been published elsewhere [14].

The canonical angular momentum of the photoelectron is $\boldsymbol{r} \times (m\boldsymbol{v} - e\boldsymbol{A})$, where m is the electron mass, $\boldsymbol{v}$ its velocity, $-e$ its charge, and $\boldsymbol{A}$ the electromagnetic vector potential. In a cylindrically symmetric system with coordinates r, θ, z, the axial component of the angular momentum, or equivalently the component of canonical momentum P_θ conjugate to the cycle coordinate θ, is conserved;

$$P_\theta = mr^2\dot{\theta} - erA_\theta(r, z) = \text{const.} \tag{4}$$

Since the magnetic field along the axis is $B_n = 2A_\theta / r$, eq. (4) can be written for two points along the beam path as

$$r_1^2\dot{\theta}_1 - r_2^2\dot{\theta}_2 = \frac{e}{2m}\left(r_1^2 B_{n1} - r_2^2 B_{n2}\right). \tag{5}$$

This is a statement of Busch's theorem. The canonical angular momentum of off-axis electrons in the longitudinal magnetic field goes into kinetic angular momentum and hence skew trajectories in regions of reduced

magnetic field. This leads to a contribution to the phase space [14,15]

$$\frac{\pi^2 e^2}{8m} r_1^4 B_n^2 = 2.17 \times 10^{-3} r_1^4 B_n^2 \text{ mm}^2 \text{ sr eV}, \quad (6)$$

where the radius is expressed in millimeters and the magnetic field is in gauss. The magnetic contribution is much larger than the phase space in the absence of the field, unless r_1, the radius at the photocathode, is quite small.

3.3. Energy analyzer acceptance

An important property of an energy analyzer is the resolving power $E/\Delta E$, where E is the pass energy and ΔE is the full width at half maximum of the energy of the analyzed beam. Both the resolving power and the acceptance phase space must be considered in comparing different analyzers and different operating energies. A suitable figure of merit for comparing energy analyzers is [14]

$$M = EA\Omega/\Delta E. \quad (7)$$

There is a trade-off between the resolving power and $A\Omega$. However, since $A\Omega$ increases faster than the resolving power decreases, M is maximized by working at the lowest possible resolving power. For a 180° spherical analyzer, the acceptance phase space is [14]

$$EA\Omega = M\Delta E = 20R^2\alpha^4\Delta E \text{ mm}^2 \text{ sr eV}, \quad (8)$$

where the mean radius of the beam path, R, is in millimeters. The envelope half-angle at the entrance to the hemispheres, α, is in radians.

4. Spin analyzers

4.1. Principle

The spin-dependent interaction which is the basis of the most commonly used spin analyzers is the spin–orbit interaction. When an electron with spin $\boldsymbol{s}$ scatters in the potential $V(r)$ of a nucleus with atomic number Z, there is an addition to the overall scattering potential which depends on the relative orientation of the incident electron spin $\boldsymbol{s}$ and its orbital angular momentum $\boldsymbol{L}$ as it scatters from the nucleus. This additional term V_{so}, the spin–orbit potential, can be written as [7]

$$V_{so} = \frac{1}{2m^2c^2}\frac{1}{r}\frac{dV}{dr}\boldsymbol{L}\cdot\boldsymbol{s}. \quad (9)$$

The spin–orbit interaction has the effect, for positive analyzing power, of making the scattering cross section larger (smaller) for electrons with spin parallel (antiparallel) to the normal $\hat{\boldsymbol{n}}$ to the scattering plane. The cross section is given by

$$\sigma(\theta) = I(\theta)[1 + S(\theta)\boldsymbol{P}\cdot\hat{\boldsymbol{n}}], \quad (10)$$

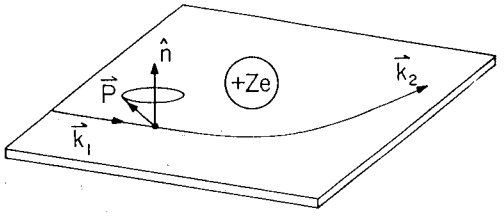

Fig. 2. Schematic of the Mott scattering geometry for an electron beam scattering from a nucleus Ze with momentum $\boldsymbol{k}_1$ and $\boldsymbol{k}_2$ before and after the scattering respectively. This geometry measures the component of the polarization $\boldsymbol{P}$ of the beam along the scattering plane normal $\hat{\boldsymbol{n}}$ (from ref. [24]).

where

$$\hat{\boldsymbol{n}} = \frac{\boldsymbol{k}_1 \times \boldsymbol{k}_2}{|\boldsymbol{k}_1 \times \boldsymbol{k}_2|},$$

with $\boldsymbol{k}_1$ and $\boldsymbol{k}_2$ the initial and final state wave vectors respectively as shown in fig. 2. The analyzing power, or Sherman function, $S(\theta)$ depends on the material, the electron energy, and scattering angle. Parity conservation demands that the polarization $\boldsymbol{P}$, which is an axial vector, be measured with respect to another axial vector, in this case $\hat{\boldsymbol{n}}$. To determine the polarization of an electron beam, one measures a spatial asymmetry A between the number of electrons scattered to the left N_L and to the right N_R from a target:

$$A = \frac{N_L - N_R}{N_L + N_R}. \quad (11)$$

From eq. (10) one can show that $A = PS$. Thus, if S is known for a given energy and scattering geometry, we can measure A to determine P.

The uncertainty in the determination of P is given by eq. (1). The figure of merit is defined as

$$\mathscr{F} = \eta S^2 = S^2 I/I_0. \quad (12)$$

Here $\eta = I/I_0$ where I is the scattered intensity in eq. (10) and I_0 is the beam intensity incident on the scattering target. The figure of merit is useful in comparing analyzers when uncertainty is limited by counting statistics.

Systematic errors may also contribute to the uncertainty in the polarization measurement. Note that eq. (11) relies on the fact that the asymmetry is due only to the spin dependence. The apparatus is assumed to be completely symmetric about a plane perpendicular to the scattering plane and containing the electron beam. The reflection symmetry about this plane includes not only geometry but also the electronics and detector sensitivity. Departures from perfect symmetry are called apparatus asymmetries. In practice there is always an apparatus asymmetry. This is not bad as long as it is stable and can be measured, for example by reversing

the polarization of an incident beam without changing anything else. A detailed discussion of this problem has been presented by Kessler [7]. Uncontrolled apparatus asymmetries, such as changes in the position or angle of the electron beam on the target, are undesirable. Such changes might be caused, for example, by reversing the magnetic field at the sample, or by movement of the synchrotron radiation beam on the sample. Care should be taken to minimize such disturbances and the electron optics must be so designed that the effect of such disturbances on the electrons reaching the scattering target of the spin analyzer produces minimal apparatus asymmetries. Ultimately the spin analyzer must not be considered in isolation but as part of the total experimental system.

The underlying theory of spin analysis was worked out by Mott in 1929 [16]. He emphasized that (1) the electron energy should be greater than 50 keV so the speed of the electron approaches the speed of light, (2) the nucleus should be of high atomic number to maximize the field gradient, and (3) the scattering angle should be greater than 90°. Such spin-dependent scattering was first observed in 1940 by Shull et al. [17]. We now know that even when the conditions set out by Mott are much relaxed, spin dependence can still be observed (although none is expected in forward scattering when $\boldsymbol{L} = 0$). For example, high incident energies are not required because low energy electrons may become relativistic on acceleration in the field of the nucleus.

One of the main differences in spin analyzers is the scattering energy which can span three orders of magnitude from 100 eV to 100 keV. The most obvious impact of the energy variation is the difference in the size of the analyzers. Less obvious but also important is that a high energy analyzer has a larger acceptance phase space and is less sensitive to target surface contamination. Also, quite different geometries are employed in the various types of spin analyzers. In some analyzers, such as retarding Mott analyzers, the scattered electrons are decelerated to detectors near ground potential. The analyzers also vary in the degree of elastic versus inelastic scattering which is detected. Finally, the targets used in different analyzers vary from thin Au films, to W single crystals, to thick polycrystalline Au films opaque to the electron beam. Four basic types of analyzers are described and compared in the next sections. Properties such as scattering energy, size, type of target, vacuum requirements, allowable energy spread, acceptance phase space $EA\Omega$, I/I_0, analyzing power, and figure of merit are collected in table 1.

A spin analyzer utilizing spin–orbit scattering from a Hg atomic beam has been developed [18] but will not be further described because of the usual requirement of ultrahigh vacuum in photoemission experiments with synchrotron radiation. Another analyzer, the absorbed current analyzer [19], takes advantage of the spin–orbit-induced spin-dependent asymmetry in the absorbed current when an electron beam is incident at an angle to a metallic surface. Since it operates only in an analog mode, and pulse counting is expected to be essential in a photoemission experiment even with undulator radiation, it will likewise not be further discussed.

4.2. Traditional Mott spin analyzer

The traditional Mott analyzer operates at an energy of 100–120 keV and at scattering angles in a range around 120°. The first spin-polarized photoemission measurements reported in 1969 [20], used the longitudinal configuration and the same type of Mott spin analyzer as continues in use at present. Energy- and angle-resolved spin-polarized photoemission measurements in the transverse geometry have also used the Mott analyzer. The experimental system has been described in detail [11,21]. The 100 keV accelerator and Mott chamber are shown in fig. 3. In this system the

Table 1
Comparison of spin analyzers

Analyzer type	Operating energy	Size [m^3]	Target	Vacuum required	ΔE	$AE\Omega$ [mm^2 sr eV]	I/I_0	S	Figure of merit	Ref.
Traditional Mott	100 keV	1–10	Thin Au foil	10^{-5}	10 keV	10^3	1.5×10^{-3}	0.26	1×10^{-4}	[11]
Retarding Mott										
spherical	30 keV	10^{-1}	Thin Au foil	10^{-5}	1.3 keV	10^4	0.7×10^{-3}	0.17	2×10^{-5}	[25]
cylindrical	100 keV	10^{-1}	Thin Au foil	10^{-5}	1.3 keV	10^4	10^{-6}	0.33	1×10^{-7}	[26,27]
Low energy electron diffraction	105 keV	10^{-3}	W crystal	10^{-10}	2 eV	1.6	2.2×10^{-3}	0.27	1.6×10^{-4}	[29]
Low energy diffuse scattering	150 eV	10^{-3}	Au film	10^{-9}	40 eV	10^2	0.9×10^{-2}	0.11	1×10^{-4}	[32]

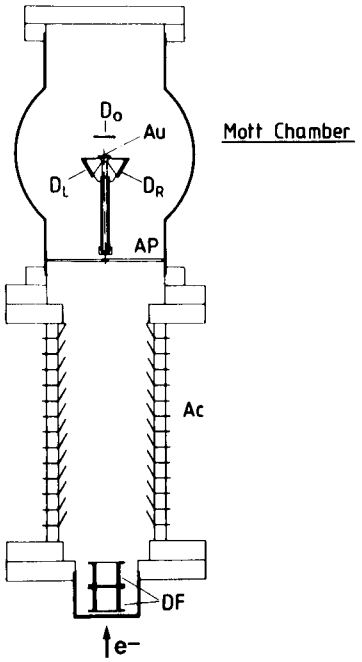

Fig. 3. The Mott spin analyzer showing deflection plates (DF) at the entrance of the 100 keV accelerator (Ac). The beam is limited by apertures (AP) before scattering from the Au foil into detectors (D_L and D_R) at 120° scattering angle. A detector D_0 in the forward direction monitors the beam (from ref. [11]).

entire Mott chamber is at 100 kV and surrounded by a safety region of a few cubic meters. Signals are optically coupled out of the high voltage region.

The calculated [22] variation in the Sherman function S and the differential scattering cross section as a function of scattering angle are shown in fig. 4. The Sherman function varies slowly in the region around 120°. Efficiency can be optimized by collecting over a range of scattering angles for examples $120° \pm 20°$ where S still remains large. Fig. 4 also gives an idea of the magnitude of apparatus asymmetry for a misaligned beam. For an angular deviation of 2° such that the scattering to the left and to the right would be 118° and 122° respectively, the variation in cross section leads to an asymmetry of 0.028 which for a typical Shermal function gives a polarization uncertainty $\Delta P \simeq 10\%$. A lateral displacement of the beam also changes the scattering angle relative to fixed electron detectors. But this effect is much smaller than the change in the solid angle subtended by the electron detectors. A change $\Delta\Omega$ in the solid angle Ω leads to a change in the asymmetry $\Delta A = \Delta\Omega/\Omega$. For a typical Mott analyzer a beam displacement of 0.1 mm leads to $\Delta P = \Delta\Omega/S\Omega \simeq 2\%$. A small Sherman function increases the effect of the apparatus asymmetry on ΔP. Note that it is the change in beam position or angle which disturb the measurement, and that a stable misalignment does not.

An interesting alternative geometry has been employed in spin polarized Auger studies [23]. Instead of a linear accelerator as in fig. 3, the acceleration takes place radially in two stages between concentric hemispheres. This fixes the beam position on the foil at the center of the spheres. Details of this analyzer, such as the figure of merit, have not been reported.

Mott analyzers are traditionally calibrated by making a comparison with theory [22] which is thought to be accurate at 100 keV. The theory is for single elastic scattering. Single scattering is approximated by using Au target foils of decreasing thickness and extrapolating to zero thickness. The Si barrier surface detectors typically used have an energy resolution of ~10 keV so care must be taken in treating inelastic scattering. Uncertainties in the functional form of the extrapolation, deriving from uncertainties in the treatment of multiple scattering, lead to a minimum one standard deviation fractional uncertainty $\Delta P/P$ in a polarization measurement of $\pm 3\%$ [24]. Considering the uncertainty in the calculation of S, it has been estimated [24] that the one standard deviation fractional uncertainty in the accuracy of absolute polarization measurement is at least $\pm 5\%$. Double scattering measurements of $|S|$ to test the theory are very difficult. Because other analyzers which operate at lower energy are usually calibrated against Mott analyzers, these uncertainties apply to them as well. Relative measurements can be made with greater precision.

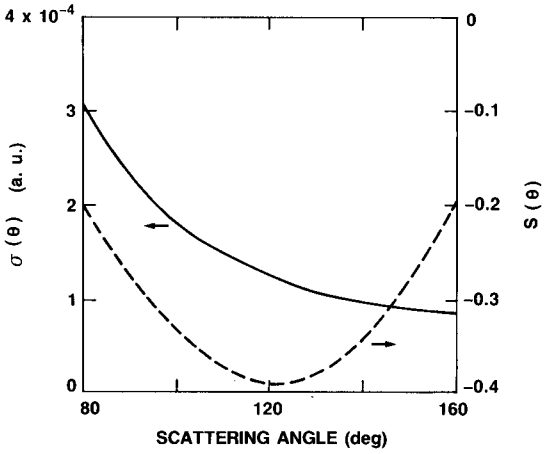

Fig. 4. The theoretical [22] differential cross section $\sigma(\theta)$ and analyzing power or Sherman function $S(\theta)$ are shown for 100 keV electron scattering from Au over a range of scattering angles of interest for spin analysis. The cross section is given in atomic units where the unit of length is the Bohr radius.

4.3. Retarding Mott analyzers

A retarding Mott analyzer [25] is shown in fig. 5. In this case the electron beam is accelerated between an outer hemispherical electrode at 1 keV to an inner hemisphere at 30 keV. The electrons are focused to a spot at the center of the sphere. The electron optical acceptance is substantial, although the angle and position constraints on the incident electron beam to maintain variations in apparatus asymmetry at an acceptable level have not been reported. After striking the Au foil target and passing out of the aperture at $\theta = 120°$ in the inner hemisphere, the electrons are decelerated as they travel to the outer hemisphere. Any transverse momentum of the electron gains in importance on deceleration and intensity is lost, thereby reducing η. However, the retarding field allows for good discrimination against inelastic electrons which may help comparisons to theory for calibration.

Retarding Mott analyzers have been realized in the cylindrical geometry [26,27] and used at 100 keV. In this geometry there is no focusing by the cylindrical field in the axial direction, further reducing η. The cylindrical analyzer is well suited for calibrating other spin analyzers because the Au foil can be moved from the beam path and the electrons are decelerated on passing to the outer cylinder and can then travel onto the analyzer being calibrated.

In retarding Mott analyzers the detectors are at low voltage and the vacuum housing is at ground potential, making them convenient to use and considerably smaller than traditional Mott analyzers, although still not easily movable. Recently a very compact movable version of this type operating at 20 keV was described [28]. Retarding analyzers have not yet been used in photoemission experiments and future applications will depend on the achievement of adequate figures of merit and control of apparatus asymmetries.

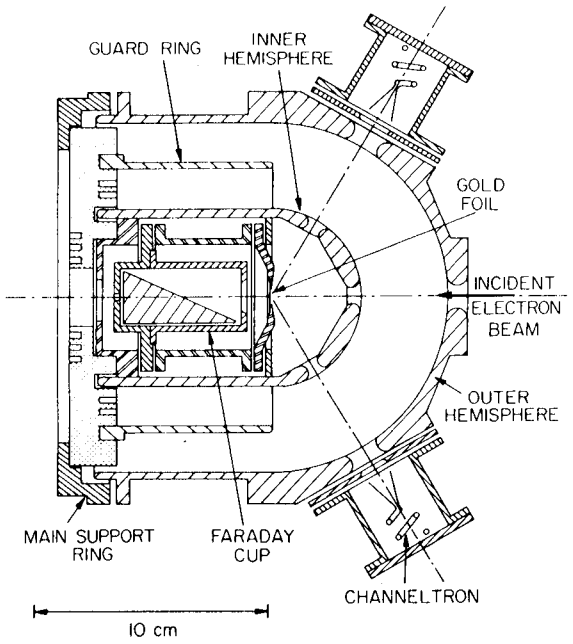

Fig. 5. Schematic of a retarding type Mott spin analyzer with hemispherical electrodes (from ref. [25]).

4.4. Low energy electron diffraction spin analyzer

In contrast to the above analyzers operating at many keV, the low energy electron diffraction (LEED) analyzer operates around 100 eV [29]. There is considerable multiple scattering from the W single crystals target. The analyzer must be calibrated against a Mott analyzer or in a double scattering experiment. The diffraction from the single crystal is exploited by detecting the scattered electrons which have been concentrated into well defined beams. The constraints on the incident beam (angular spread less than 2° and energy spread less than 5 eV) are quite severe but should not be a limitation in a spin-polarized photoemission experiment where such energy and angular resolution are wanted. The LEED spin analyzer may be less suitable for an experiment in the longitudinal configuration, depending on the constraints imposed by the energy analyzer. This spin analyzer was used in preliminary angle-resolved spin-polarized photoemission from W [30] and subsequently in some detailed studies of Pt [31].

The figure of merit of the spin analyzer is high, although one should be aware of the constraints on the incident beam which could reduce the acceptable incident beam current I_0. As with any spin analyzer, if information-carrying electrons must be rejected before reaching the analyzeer, a high I/I_0 producing a high figure of merit could be misleading.

The LEED spin analyzer is compact and, for beams already well defined in energy and angle, has a high figure of mert. The main drawback is the requirement that the W target be atomically clean which requires flashing to ~ 2500 K every quarter to half hour [29]. The alignment of the crystal in the analyzer is also critical.

4.5. Low energy diffuse scattering spin analyzer

A new type of spin analyzer was introduced recently [32]. Like the LEED analyzer it operates at low energy, ~ 150 eV, and requires an initial calibration with a high energy Mott analyzer. It employs an evaporated polycrystalline Au film which is opaque to the incident electron beam. The target is very stable and reproducible. The fact that the scattering is diffuse and into a large solid angle reduces the intensity at any one angle

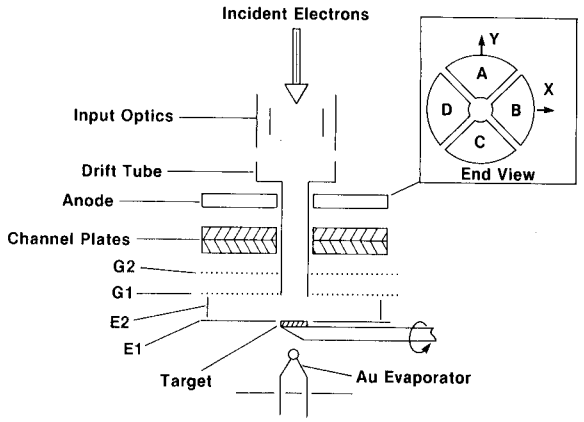

Fig. 6. Schematic of the low-energy diffuse scattering spin analyzer. The inset shows the view of the anode seen by electrons emerging from the channel plate (from ref. [32]).

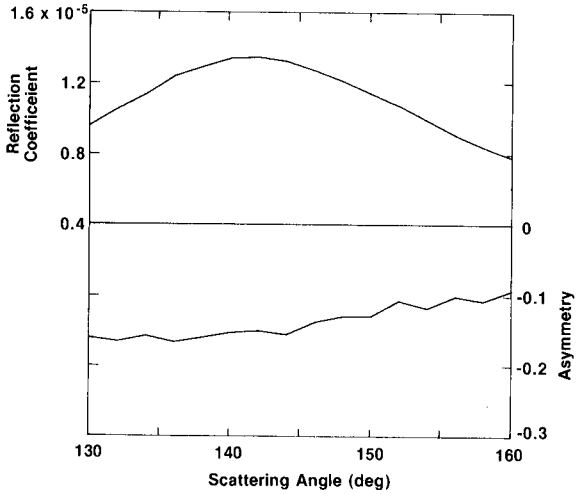

Fig. 7. Angular dependence of the intensity and of the spin dependent asymmetry for scattering 145 eV electrons from a polycrystalline Au film (from ref. [32]).

drastically; this is compensated for by collecting over a large solid angle. Since diffraction conditions do not have to be met, the constraints on the range of incident angles and beam energies are greatly relaxed. It is compact and movable and generally well suited to an angle- and energy-resolved spin-polarized photoemission experiment.

The low-energy diffuse-scattering spin analyzer is shown schematically in fig. 6. The electron beam passes through a drift tube to the Au target. The electrons are diffusely scattered into the field-free region formed by electrodes E_1 and E_2 and by grid G_1. A retarding voltage on grid G_2 prevents very low energy secondaries generated at the Au target, which do not retain the polarization information, from reaching the channel plates. The signal is amplified by the microchannel plate multiplier assembly. The electrons exciting the channel plate are collected by the sectored anode shown in the inset of fig. 6. The four quadrants allow simultaneous measurement of the two transverse polarization components. For example,

$$P_x = \frac{1}{S}\frac{N_A - N_C}{N_A + N_C}, \tag{13}$$

where N_A and N_C are the numbers of electrons measured at anode A and C respectively.

The analyzing power and reflection coefficient for a 145 eV beam of electrons incident on an evaporated Au film are shown in fig. 7. The reflection coefficient was measured for elastic scattering into a Faraday cup detector with entrance cone half-angle of 1°. These curves, like those in fig. 4 for the high energy Mott analyzer show the sensitivity of S and η to the scattering angle. Not shown in fig. 7 is the large backscattering peak near $\theta = 180°$. The integrated analyzing power for the analyzer shown in fig. 6 is $S = 0.11$. This is very stable in ultrahigh vacuum and was found to decrease by 10% only after 3×10^4 langmuir exposure to an intentional air leak. The Au target is readily regenerated by reevaporation.

The acceptance phase space of the analyzer depicted in fig. 6 is quite large. An acceptance half-angle of 10° and an area of 16 mm^2 produce an $EA\Omega$ of order 100 mm^2 sr eV. This large acceptance phase space is only useful if it is filled or if the incident beam is very stable within it. Thus, an electron beam which varied in angle and position would still reach the scattering target but could also lead to an intolerable variation of apparatus asymmetry. It is the job of the input optics, shown schematically in fig. 6, to couple the spin analyzer to the rest of the experiment and constrain the beam to avoid any significant variation in apparatus asymmetry. This spin analyzer is now being tested in a spin polarized photoemission experiment on the U5 beam line at the Brookhaven National Synchrotron Light Source. It has been installed after the exit optics of a movable hemispherical energy analyzer. Preliminary results indicate that displacements of the synchrotron radiation beam on the sample introduce spin analyzer apparatus asymmetries [33]. Work is in progress to control radiation movement or to eliminate the effect of it on the spin analyzer.

5. Conclusion

The importance of analyzing the total experimental system to determine the appropriateness of a spin analyzer has been emphasized. Factors such as the figure of merit have to be taken into account in connection with the acceptance phase space, stability, size, etc. To summarize, two specific examples will be discussed.

First, consider an energy- and angle-resolved spin-polarized photoemission experiment in the transverse configuration using a hemispherical energy analyzer with $R = 50$ mm, $\alpha = 4°$, and $\Delta E = 0.1$ eV. From eq. (8), one obtains for the energy analyzer acceptance, $EA\Omega = 0.12$ mm^2 sr eV, a value which is much smaller than the acceptance phase space of any of the spin analyzers considered. Other criteria in our selection of a spin analyzer would be figure of merit, and certainly for this application, compactness and movability. Ideally one wants a spin analyzer than can be connected to the output of an energy analyzer much like a channeltron. For energy- and angle-resolved spin-polarized photoemission, we have chosen the low-energy diffuse-scattering analyzer with its high figure of merit and easily prepared and stable scattering target.

Second, consider the same energy analyzer in the longitudinal configuration with $B = 1$ kG. From eq. (6) we find that only electrons emitted from within a spot 0.17 mm in diameter will be accepted by the energy analyzer. For such measurements, energy analyzers with higher acceptance should be used, noting that angular resolution is not required in the longitudinal configuration. The larger photocathode emittance of the longitudinal configuration has so far limited "energy-resolved measurements" to the vicinity of the photothreshold [1] or to retarding field analysis [34]. With new synchrotron radiation sources, energy-resolved spin-polarized photoemission will be possible at reasonable energy resolution in the longitudinal configuration with dispersive energy analyzers. Because compactness is not such an advantage as it is in the angle resolved measurement, a high-energy Mott analyzer is favored for measurements in the longitudinal configuration. The large acceptance phase space of the spin analyzer would put no constraints on the phase space of the energy analyzer. Recalling that $r\alpha\sqrt{E}$ is a conserved quantity, we see that $r\alpha$ is about 30 times smaller for a high-energy Mott analyzer than for a low-energy spin analyzer. Thus, apparatus asymmetries resulting from changes in beam alignment are minimized, which is important when large magnetic fields are being switched at the sample.

The spin analyzers discussed above each have special attributes which can be selected for a particular application. The fact remains that of order 10^4 times more signal is still required for a polarization measurement than for an intensity measurement of comparable precision. However, with new high-brilliance sources of synchrotron radiation we expect spin-polarized photoemission experiments to become more commonplace and to open up new and exciting scientific opportunities.

Acknowledgements

Helpful discussions with C.E. Kuyatt are gratefully acknowledged. This work was supported in part by the Office of Naval Research and NSF Grant DMR-86-03304.

References

[1] H.C. Siegmann, F. Meier, M. Erbudak and M. Landolt, Adv. Electron. Electron Phys. 62 (1984) 1; S.F. Alvarado, W. Eib, F. Meier, H.C. Siegmann and P. Zurcher, in: Photoemission and Electronic Properties of Surfaces, eds., B. Feuerbacher, B. Fitton and R.F. Willis (Wiley, New York, 1978) p. 437.
[2] E. Kisker, K. Shröder, W. Gudat and M. Campagna, Phys. Rev. B31 (1985) 329.
[3] R. Clauberg, H. Hopster and R. Raue, Phys. Rev. B29 (1984) 4395.
[4] L.E. Klebanoff, S.W. Robey, G. Liu and D.A. Shirley, Phys. Rev. B30 (1984) 1048.
[5] A.S. Arrott, B. Heinrich, S.T. Purcell, J.F. Cochran and K.B. Urquhart, J. Appl. Phys. 61 (1987) 3721.
[6] C.L. Fu, A.J. Freeman and T. Oguchi, Phys. Rev. Lett. 54 (1985) 2700.
[7] J. Kessler, Polarized Electrons, 2nd ed. (Springer, Berlin, 1985).
[8] A. Arko, S.D. Bader, C.T. Chen, M. Knotek, E.W. Plummer, N.V. Smith and J. Stohr, Soft X-ray Applications of the Advance Photon Source, in: Report of the Workshop on the Scientific Case of the 6 GeV Synchrotron Source, Argonne National Laboratory (1985).
[9] J. Unguris, G. Hembree, R.J. Celotta and D.T. Pierce, J. Mag. Mag. Mater. 54–57 (1986) 1629.
[10] R.J. Celotta, D.T. Pierce, G.C. Wang, S.D. Bader and G.P. Felcher, Phys. Rev. Lett. 43 (1979) 728.
[11] E. Kisker, R. Clauberg and W. Gudat, Rev. Sci. Instr. 53 (1982) 1137.
[12] D.T. Pierce, R.J. Celotta, J. Unguris and H.C. Siegmann, Phys. Rev. 26 (1982) 2566.
[13] P.A. Sturrock, Static and Dynamic Electron Optics (Cambridge University Press, New York, 1955) chap. 2.
[14] D.T. Pierce, C.E. Kuyatt and R.J. Celotta, Rev. Sci. Instr. 50 (1979) 1467.
[15] V.W. Hughes, R.L. Long Jr., M.S. Lubell, M. Posner and W. Raith, Phys. Rev. A5 (1972) 195.
[16] N.F. Mott, Proc. Roy. Soc. (London) A124 (1929) 425; A135 (1932) 429.
[17] L.G. Schull, C.T. Chase and F.F. Myers, Phys. Rev. 63 (1943) 29.
[18] K. Jost, F. Kaussen and J. Kessler, J. Phys. E14 (1981) 735.
[19] D.T. Pierce, S.M. Girvin, J. Unguris and R.J. Celotta, Rev. Sci. Instr. 52 (1981) 1437; M. Erbudak and G. Ravano, J. Appl. Phys. 52 (1981) 5032.
[20] G. Busch, M. Campagna, P. Cotti and H.C. Siegmann, Phys. Rev. Lett. 22 (1969) 597.
[21] R. Raue, H. Hopster and E. Kisker, Rev. Sci. Instr. 55 (1984) 383.
[22] G. Holzwarth and H.J. Meister, Tables of Asymmetry, Cross Sections and Related Functions for Mott Scattering of Electrons by Screened Au and Hg Nuclei (University of Munich, Munich 1964).
[23] M. Landolt, R. Allenspach and D. Mauri, J. Appl. Phys. 57 (1985) 3626.

[24] G.D. Fletcher, T.J. Gay and M.S. Lubell, Phys. Rev. A34 (1986) 911.
[25] L.G. Gray, M.W. Hart, F.B. Dunning and G.K. Walters, Rev. Sci. Instr. 55 (1984) 88.
[26] L.A. Hodge, T.J. Moravec, F.B. Dunning and G.K. Walters, Rev. Sci. Instr. 50 (1979) 5.
[27] D.M. Campbell, C. Hermann, G. Lampel and R. Owens, J. Phys. E18 (1985) 664.
[28] F.B. Dunning, L.G. Gray, J.M. Ratcliff, F.C. Tang, X. Zhang and G.K. Walters, Rev. Sci. Instr. 58 (1987) 1706.
[29] J. Kirschner and R. Feder, Phys. Rev. Lett. 42 (1979) 1008; J. Kirschner, Polarized Electrons at Surfaces (Springer, Berlin, 1985) p. 62.
[30] J. Kirschner, R. Feder and J.C. Wendelken, Phys. Rev. Lett. 47 (1981) 614.
[31] A. Eyers, F. Schäfers, G. Schönhense, U. Heinzmann, H.P. Oepen, K. Hünlich, J. Kirschner and G. Borstel, Phys. Rev. Lett. 52 (1984) 1559.
[32] J. Unguris, D.T. Pierce and R.J. Celotta, Rev. Sci. Instr. 57 (1986) 1314.
[33] P.D. Johnson, S.D. Hubert, B. Sinkovic, N. Brookes, R. Klaffy, private communication.
[34] W. Gudat, E. Kisker, E. Kuhlmann and M. Campagna, Solid State Commun. 37 (1981) 771.